A comparative study of electronic, structural, and magnetic properties of α-, β-, and γ-$Cu_2V_2O_7$

S. Bhowal,[1] J. Sannigrahi,[1] S. Majumdar,[1] and I. Dasgupta[1,2,*]

[1]*Department of Solid State Physics, Indian Association for the Cultivation of Science, 2A & B Raja S. C. Mullick Road, Jadavpur, Kolkata 700 032, India*

[2]*Centre for Advanced Materials, Indian Association for the Cultivation of Science, Jadavpur, Kolkata-700032, India*

(Received 10 June 2016; revised manuscript received 5 December 2016; published 3 February 2017)

We have carried out a detailed first-principles study of the copper pyrovanadate $Cu_2V_2O_7$ which crystallizes in at least three different polymorphs α, β, and γ. The magnetic properties of these systems are analyzed by calculating various exchange interactions and deriving the relevant spin Hamiltonian. Our detailed analysis based on the derived spin model suggests the crucial role of the crystal structure in governing the electronic and magnetic properties of the three different phases of the system. In particular, our calculations reveal that a subtle difference in the crystal structure has a substantial impact on the magnetic properties of the α phase. The important role of spin-orbit coupling (SOC) is also investigated for the three different phases of $Cu_2V_2O_7$. Although SOC stabilizes magnetic order in all the phases, the absence of inversion symmetry leads to an appreciable Dzyaloshinski-Moriya interaction in the α phase which in turn causes the canting of the spins and adds to the stabilization of the long-range order. Finally, from the symmetry analysis and total energy calculation we have obtained the magnetic ground state for the different phases of $Cu_2V_2O_7$. While the symmetry-allowed magnetic ground states for the α and β phases are in agreement with the experimental observations, the theoretically predicted magnetic ground state for the γ phase is found to be a realization of a dimeric system with the potential to host novel physics.

DOI: 10.1103/PhysRevB.95.075110

I. INTRODUCTION

Low-dimensional quantum spin systems have attracted considerable attention both theoretically as well as experimentally because of the wealth of fascinating properties exhibited by them [1]. Copper based compounds have received special interest due to their proximity to the superconducting two-dimensional cuprates. In this respect, copper divanadates ($Cu_2V_2O_7$) have attracted great interest, especially because of the fascinating electronic and magnetic properties observed in different phases of the compound. $M_2X_2O_7$ compounds broadly crystallize in two different groups of structures: thortveitite ($Sc_2Si_2O_7$) and dichromate ($K_2Cr_2O_7$). The difference between the two structures depends on the X-O-X angle. While in the thortveitite structure the angle is 180°, for the dichromate structure it deviates from 180° [2]. The compound $Cu_2V_2O_7$ crystallizes in dichromate structure with at least three different polymorphs, namely, (i) α phase which is orthorhombic, (ii) β phase which is monoclinic, and (iii) γ phase which crystallizes in triclinic structure [3–5]. Out of these three phases, the crystal structure of the α phase is noncentrosymmetric, while the structures of the other two are centrosymmetric.

The high temperature polymorph γ-$Cu_2V_2O_7$ transforms to the low temperature α and β phases depending upon the cooling rate [6]. However, it should be noted that, at ambient conditions α-$Cu_2V_2O_7$ is the only stable phase, whereas both β and γ phases are metastable. Interestingly, the substitution of nonmagnetic Zn^{2+} ion in place of the Cu^{2+} ion induces a polymorphic transition from the α phase to the β phase which in turn has a pronounced effect on the magnetism of the system [7]. The electronic and magnetic properties of α and β phases are found to be quite intriguing, while there are not many experimental reports available for the γ phase. Investigations on α-$Cu_2V_2O_7$ reveal that it undergoes a transformation to a long-range magnetically ordered state below $T_C = 35$ K with a canted antiferromagnetic (AFM) type magnetic order [8]. Our previous combined theoretical and experimental work [9] on the polycrystalline sample of α-$Cu_2V_2O_7$ established the compound to be a magnetic multiferroic with giant electric polarization (0.55 $\mu C/cm^2$) below T_C. The α phase is an antiferromagnet with dominant AFM third nearest-neighbor exchange interaction J_3. In addition, strong Dzyaloshinski-Moriya (DM) interaction leads to canting of spins promoting weak ferromagnetism in the magnetically ordered state. α-$Cu_2V_2O_7$ is found to be the only multiferroic material among various divanadates ($M_2V_2O_7$) where the origin of giant ferroelectric polarization is attributed to the symmetric exchange-striction mechanism. However, a recent study by Gitgeatpong *et al.* [10] on the single crystal α-$Cu_2V_2O_7$ proposed a helical-honeycomb spin network with dominant first and second nearest-neighbor interaction J_1 and J_2, respectively. Another study by Lee *et al.* [11] on the single crystal of α-$Cu_2V_2O_7$ argued that the system is pyroelectric rather than ferroelectric both above and below T_N. On the other hand, the β phase exhibits the low-dimensional character of its spin system. The compound shows a broad humplike feature in its magnetic susceptibility around 50 K and eventually shows an antiferromagnetically ordered ground state below $T_N = 26$ K [2,12]. There are several proposals in the literature regarding the spin model for the β phase of the compound. While Yashima *et al.* [13] proposed a spin chain model, a detailed study by Tsirlin *et al.* [4] showed that β-$Cu_2V_2O_7$ could be the best available experimental realization of the spin-1/2 Heisenberg model on the honeycomb lattice. There are hardly any experimental or theoretical studies on the γ phase of the system.

*sspid@iacs.res.in

In the present paper we have carried out a comparative study of the α, β, and γ phases of $Cu_2V_2O_7$ using first-principles electronic structure calculations based on density functional theory (DFT). In order to understand the magnetism in the three phases of $Cu_2V_2O_7$, we have identified the dominant exchange paths and derived the relevant spin Hamiltonian. In particular, we show that a subtle difference in the crystal structure has a substantial impact on the magnetic properties of the α phase providing a clue to understanding the origin of discrepancy in the magnetic properties reported by various groups. We have investigated the importance of spin-orbit coupling (SOC) on the magnetic properties and also calculated the probable magnetic ground states for the polymorphs from symmetry-allowed magnetic configurations. The remainder of the paper is organized as follows. In Sec. II, we discuss the crystal structure of the three phases and present our computational techniques in detail. Section III is devoted to results and discussions followed by the conclusions in Sec. IV.

II. CRYSTAL STRUCTURE AND COMPUTATIONAL DETAIL

As described earlier, α-, β-, and γ-$Cu_2V_2O_7$ crystallizes in the orthorhombic space group $Fdd2$ [3,9] [see Table I of the Supplemental Material (SM) [14] for structural parameters used in the present calculation], the monoclinic space group $C2/c$ [15,16], and the triclinic space group $P\bar{1}$ [5], respectively. The top panel of Fig. 1 shows the conventional unit cell of the α, β, and γ phases, respectively.

All three phases consist of magnetic Cu^{2+} ($3d^9, S = \frac{1}{2}$) and nonmagnetic V^{5+} ($3d^0$, $S = 0$) metal ions making them a system having both partially filled and empty d shells. All the equivalent Cu^{2+} ions in the α and β phases are in fivefold coordination (better described by $4 + 1$) to oxygen atoms forming a distorted [CuO_5] polyhedron (pyramids) as shown in the bottom panel of Fig 1. The distortion in the [CuO_5] polyhedron is found to be much pronounced in the α phase (with Cu-O bond length 1.88–1.98 Å, and 2.55 Å) than in the β phase (having Cu-O bond length 1.93–1.95 Å, and 2.26 Å). These CuO_5 pyramids share their edges and thereby form chains parallel to [011] and [01$\bar{1}$] in the α phase and [110] and [1$\bar{1}$0] in the β phase, respectively.

On the contrary, the structure of the γ phase contains two inequivalent Cu^{2+} ions. The Cu(1) atom is in a distorted octahedral environment with four smaller equatorial Cu-O bonds (1.91–2.0 Å) and two longer apical bonds (2.42–2.54 Å), while the Cu(2) atom is in fivefold coordination ($4 + 1$) to the oxygen atom with four smaller bond lengths (1.91–1.99 Å) and one larger bond length (2.35 Å) as shown in the bottom panel of Fig 1. These two polyhedra share their edges to form two types of chains, one of which is composed of edge sharing $Cu(1)O_6$ octahedra, whereas the other is made of edge sharing $Cu(2)O_5$ square pyramids. The orientations of the chains are also different in the three phases as shown in the middle panel of Fig. 1. In the α phase the chains are perpendicular to each other and also the plane containing the chains is oriented in the perpendicular direction. In the β phase, though, the chains are perpendicular to each other; they are in the same plane. In the

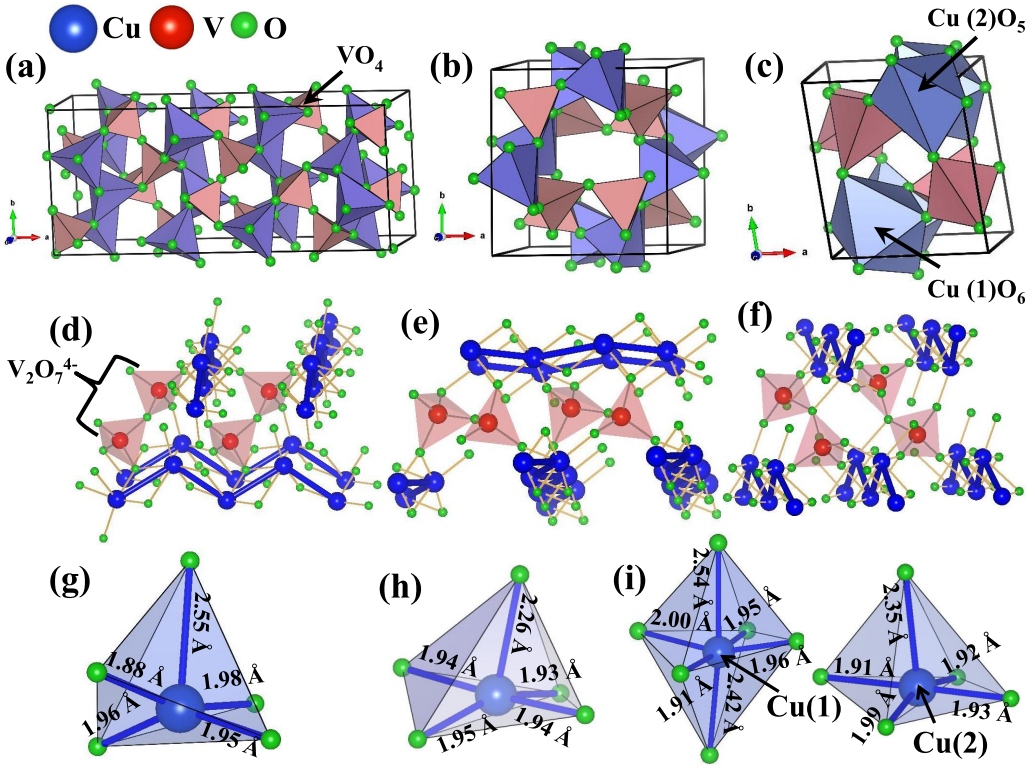

FIG. 1. Crystal structure of (a) α-, (b) β-, and (c) γ-$Cu_2V_2O_7$ (top panel). The different orientations of the Cu-Cu chain in these three phases are shown in (d), (e), and (f), respectively (middle panel). The copper polyhedra for the (g) α, (h) β, and (i) γ phases (bottom panel). See text for details.

γ phase, the chains as well as the plane containing the chains are parallel to each other.

In all the polymorphs of $Cu_2V_2O_7$, the Cu chains are separated by the $V_2O_7^{4-}$ anionic group which results from two corner sharing VO_4 tetrahedra as marked in the middle panel of Fig 1. The VO_4 tetrahedra are found to be much more distorted in the γ phase (1.66–1.84 Å) than in the α (1.65–1.74 Å) and the β phases (1.64–1.78 Å). The V-O-V angles for the α, β, and γ phases are, respectively, 147.83(19)° (which is in very good agreement with Refs. [3,17]), 131.97(8)° [15,16], and 134.84(18)° [5].

It is very important to note that the V-O-V angle [2,3] plays a crucial role in deciding the exchange path for the α phase which is discussed in detail in the next section. In our work [9] on the α phase, we found the V-O-V angle to be close to 148.0° from the refinement of x-ray diffraction data at room temperature which compares well with the previously reported data at room temperature on this phase [3,17]. However, in the recent [10] study on the single crystal sample of α-$Cu_2V_2O_7$, the V-O-V angle is found to deviate substantially from 148°. A possible reason for this deviation may be the presence of impurity phases in the single crystal structure of α-$Cu_2V_2O_7$ [10], or maybe the system is assuming a slightly different structure in its single crystalline form.

In order to study the electronic as well as magnetic properties of the three different phases of $Cu_2V_2O_7$, first-principles DFT calculations have been performed using the plane-wave based projector augmented wave [18,19] method as implemented in the Vienna *ab initio* simulation package (VASP) [20,21]. Exchange and correlation effects are treated within local density approximation (LDA) including Hubbard U [22] and SOC. Symmetry has been switched off in order to minimize possible numerical errors. The kinetic energy cutoff of the plane-wave basis was chosen to be 550 eV and a Γ-centered $8 \times 8 \times 8$ k mesh has been used for Brillouin zone integration for the α phase of the compound, while an $8 \times 8 \times 4$ k mesh is used for the β and γ phases of the compound.

The hopping parameters as well as on-site energies of the low-energy tight-binding model retaining only the Cu atoms in the basis are obtained from the muffin-tin orbital (MTO) based Nth order MTO (NMTO) method [23–25] as implemented in the STUTTGART code as well as by constructing the Wannier function using the VASP2WANNIER and the WANNIER90 codes [26].

III. RESULTS AND DISCUSSIONS

A. Nonspin polarized electronic structure

To begin with we have investigated the electronic structure of the three phases of $Cu_2V_2O_7$ without magnetic order. For all three phases, the Fermi level (E_F) is dominated by an isolated manifold of four bands which arises from the four Cu atoms in the primitive unit cell containing 2 f.u. of the compound. The plot for the density of states (DOS) for the three phases (see Fig. 2) shows that O-p states are completely occupied while the Fermi level is dominated by the Cu-d states. The empty V-d states lie above the Fermi level, and the DOS is consistent with the $Cu_2^{2+}V_2^{5+}O_7^{2-}$ nominal ionic formula.

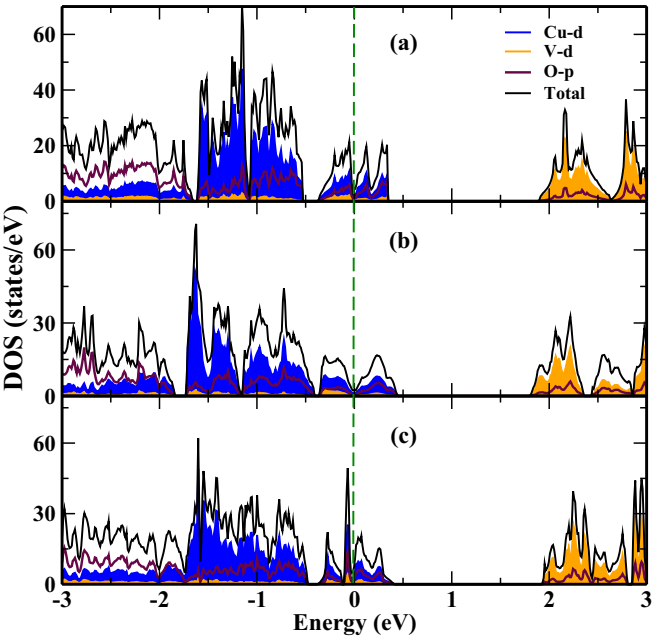

FIG. 2. Total and partial density of states (DOS) for the Cu-d, V-d, and O-p orbital are shown for (a) α-, (b) β-, and (c) γ-$Cu_2V_2O_7$ in the top, middle, and bottom panels, respectively.

We have employed the NMTO downfolding method [23–25] and the VASP2WANNIER and the WANNIER90 codes [26] to construct a low-energy, few band tight-binding model Hamiltonian for these systems. The various hoppings obtained using these methods will determine the dominant exchange paths. Here we have retained the Cu-$d_{x^2-y^2}$ orbitals in the basis for the α and β phases and downfolded the rest. The downfolded bands are plotted in Figs. 3(a) and 3(b), respectively, and we note that the agreement with the full band structure is good justifying our low-energy model Hamiltonian.

The situation is, however, different for the γ phase. The two inequivalent Cu atoms, namely, Cu(1) and Cu(2), being in different environments in the γ phase, two different orbitals primarily contribute to the bands across the Fermi level. In order to understand the contribution of the various Cu-d levels in γ-$Cu_2V_2O_7$, we have first constructed a Cu-d only low-energy Hamiltonian by integrating out all the

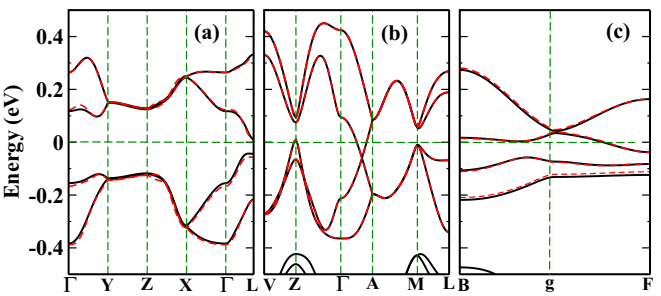

FIG. 3. Downfolded band structure (shown by red dashed lines) compared to the full orbital band structure (shown by black solid lines) for (a) α-, (b) β-, and (c) γ-$Cu_2V_2O_7$ are shown.

TABLE I. Hopping integrals (t_i) and exchange interactions (J_i) obtained from WANNIER90 for the three polymorphs of $Cu_2V_2O_7$. The reported values (Ref. [4]) are shown within parentheses for the β phase.

System	Distance (Å)	Hopping path (t_i)	Hopping (meV)	$J_i^{\rm AFM} = 4t_i^2/U_{\rm eff}$ ($U_{\rm eff} = 6.5$ eV) (meV)
	3.14	t_1	79	3.9
	3.98	t_2	11	0.1
α-$Cu_2V_2O_7$	5.27	t_3	92	5.1
	5.30	t_{4a}	16	0.2
	5.30	t_{4b}	5	0.02
	5.42	t_5	14	0.12
	5.54	t_6	31	0.6
	2.95	t_1	146 (148)	13.1
	3.26	t_2	33 (36)	0.7
β-$Cu_2V_2O_7$	4.64	t_3	17	0.2
	4.82	t_4	18	0.2
	5.18	t_5	97 (97)	5.8
	5.25	t_6	80 (84)	3.9
	2.97	t_1	111	7.6
	2.99	t_2	82	4
γ-$Cu_2V_2O_7$	3.11	t_3	17	0.2
	3.20	t_4	148	13.6
	4.46	t_5	0.5	0.2
	4.50	t_6	30	0.6
	4.60	t_7	21	0.3

high-energy degrees of freedom other than Cu-d states. From the eigenvectors (see Sec. II of the SM [14]) corresponding to the highest-energy eigenvalues, we conclude that in the global frame of reference in spite of mixed character, the Cu-d_{xz} and $d_{x^2-y^2}$ orbitals primarily contribute to the bands for Cu(1) and Cu(2), respectively, close to the Fermi level. The orthorhombic (Q_2) and tetragonal (Q_3) distortion of the Cu(1)O_6 octahedron promotes the Cu(1)-d_{xz} ($d_{x^2-z^2}$ in local frame) state close to the Fermi level [27]. This is further reflected in the plot of partial DOS for the γ phase as shown in Fig. 1 of the SM [14]. Finally, we have downfolded all the bands in the γ phase retaining only these two orbitals in the basis [see Fig. 3(c)] in order to extract the low-energy tight-binding model for the system.

Table I shows the various dominant effective hopping integrals t_{ij} between Cu ions at sites i and j for α, β, and γ phases obtained using the VASP2WANNIER and WANNIER90 methods and are consistent with that obtained using the NMTO downfolding method (see Table II of the SM [14]). The calculated hoppings for the β phase are found to be in excellent agreement with the previously reported values [4] (see the values within parentheses in Table I). It is clear from Table I that for the α phase the dominant hopping is t_3 followed by first nearest-neighbor hopping t_1, whereas for the β phase the strongest hopping is t_1 followed by t_5 and t_6. On the other hand, for the γ phase, hoppings at the first and fourth nearest-neighbors are found to be dominant.

B. Calculation of isotropic exchange interaction

To obtain insights into the magnetic properties of $Cu_2V_2O_7$, we have calculated the spin polarized DOS for the three polymorphs of $Cu_2V_2O_7$ in the ferromagnetic configuration using the LDA+U method as shown in Fig. 2 of the SM [14]. As expected for Cu^{2+}, in d^9 configuration, the majority Cu-d spin states are completely occupied while the minority spin channel is only partly occupied. In the absence of degeneracy due to structural distortion, the inclusion of Hubbard U promotes a gap in the minority spin channel lending the system to be an insulator. Next we have identified the various exchange paths guided by the hopping strengths and calculated the dominant exchange interactions. For this purpose, we have performed total energy calculations in the framework of local spin density approximation with a Hubbard U correction (LSDA+U) [22] for various ordered spin states. The relative energies of these ordered spin states, determined from the LSDA+U calculations, are then mapped onto the corresponding energies obtained from the total spin exchange energies of the Heisenberg spin Hamiltonian $H = -\sum_{ij} J_{ij}\vec{S}_i \cdot \vec{S}_j$, where $J_{ij} < 0$ implies an AFM ground state, while $J_{ij} > 0$ indicates a ferromagnetic ground state. The constrained DFT calculations by Anisimov *et al.* [22] for $CaCuO_2$ gives $U_{\rm eff} = 6.5$ eV for the Cu ions when Cu is in the 2+ charge state. Since Cu, in the present systems, are also in the same charge state, we have chosen $U_{\rm eff}$ to be 6.5 eV to estimate the exchange coupling J_{ij}. The dominant exchange interactions for the three phases are listed in Table II.

As is clear from Table II, AFM exchange J_3 is the leading interaction for the α phase followed by AFM interaction J_1 and ferromagnetic (FM) interaction J_2 [see Fig. 4(a)]. The dominant AFM exchange interaction J_3 is mediated via the Cu-O-V-O-Cu path which is also reflected in the plot of the Cu-$d_{x^2-y^2}$ Wannier function for the α phase [see Fig. 4(d)]. It is clear from this plot that the Cu-$d_{x^2-y^2}$ orbital forms a strong $pd\sigma$ antibonding state with the neighboring O-p orbitals. The tail of the Wannier function near V indicates the strong hybridization with the V atom which mediates the interaction J_3 in the α phase. The importance of J_3 is also emphasized in a recent inelastic neutron scattering study [28]. The value of Curie-Weiss temperature Θ_{CW} in the mean-field

TABLE II. Leading exchange interactions obtained from total energy calculation within LSDA+U formalism with $U_{\rm eff} = 6.5$ eV for three different polymorphs of $Cu_2V_2O_7$.

Exchange interaction J_i (meV)	α-$Cu_2V_2O_7$	Exchange interaction J_i (meV)	β-$Cu_2V_2O_7$	Exchange interaction J_i (meV)	γ-$Cu_2V_2O_7$
J_1	−4.7	J_1	−20.2 (−19.6)	J_1	−2.6
J_2	4.1	J_5	−8.0 (−9.3)	J_4	−30.7
J_3	−13.6	J_6	−11.5 (−10.8)	J_7	3.7

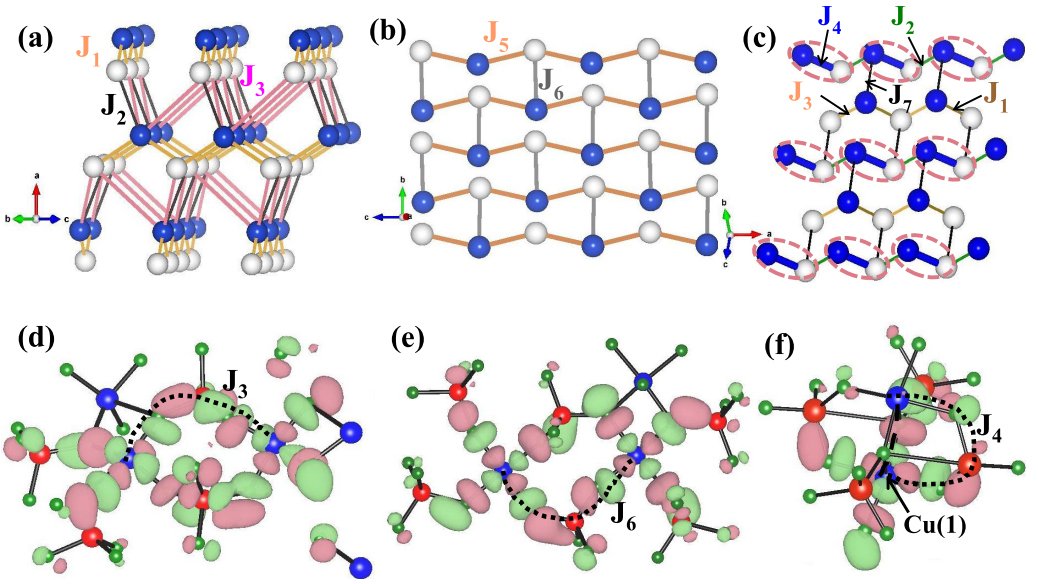

FIG. 4. Spin models for (a) α-, (b) β-, and (c) γ-$Cu_2V_2O_7$. Blue (dark) and white (light) balls represent the up and down spins (ignoring canting) at the Cu sites corresponding to the magnetic ground state. Cu(1) atoms in the γ phase at the fourth nearest neighbor form dimer as marked by the dotted line. The Wannier function plot showing the dominant exchange path for (d) α-, (e) β-, and (f) γ-$Cu_2V_2O_7$. Cu, V, and O atoms are indicated in blue, red, and green.

limit using the exchange interactions presented in Table II for α-$Cu_2V_2O_7$ is calculated to be -77.38 K in good agreement with the experimental value (-77.8 K) justifying the reliability of our calculated exchange interactions.

We gather from Table II, the dominant exchange interactions for the β phase are J_1, J_5, and J_6. These values of the exchange interactions are in good agreement with the VASP results reported in Ref. [4] (see the values within parentheses in Table II). It is, however, argued in Ref. [4] that the choice of double counting correction (DCC) in the LSDA+U method is crucial to determine the magnitude of the exchange interactions. Accordingly, using around mean field (AMF) as DCC, the nearest-neighbor exchange interaction for the β phase was reported in Ref. [4] to become very small, in comparison to J_5 and J_6 which is also observed in our AMF calculation using the full potential augmented plane-wave method as implemented in WIEN2K [29,30]. Our calculated values of these exchange parameters within LSDA+U using AMF as DCC are, respectively, $J_1 = -2.2$ meV, $J_5 = -9.8$ meV, and $J_6 = -7.2$ meV. Thus we can see that while the nearest-neighbor interaction gets substantially reduced, J_5 and J_6 form the anisotropic honeycomb spin network as shown in Fig. 4(b). The exchange interaction J_6 is mediated via the Cu-O-V-O-Cu path as also shown in the Wannier function plot for the Cu-$d_{x^2-y^2}$ orbital [see Fig. 4(e)]. As shown in Fig. 4(e), the Cu-$d_{x^2-y^2}$ orbital forms strong $pd\sigma$ antibonding states with the neighboring O-p orbital which further hybridizes with the V atom, indicated by the tail of the Wannier function near V and thereby mediates the interaction. In view of the above we have recalculated the exchange interactions of the α phase with AMF as DCC and found that J_3 is still the dominant exchange interaction.

It is very important to note that for α-$Cu_2V_2O_7$, the strengths of magnetic interactions are very sensitive to the crystal structure, in particular the V-O-V angle [2,3] (see Fig. 5). If the V-O-V angle decreases, then not only the average V-O bond length increases but also the asymmetry in the V-O bond length within the VO_4 tetrahedra increases. This further enhances the asymmetry in the two bridges Cu-O-V-O-Cu making the third nearest-neighbor hopping t_3 weaker. Again with the expansion of VO_4 tetrahedra, CuO_5 polyhedra shrink, resulting in the increase of $\angle$ Cu-O(2)-Cu reflected in the increase of the strength of the nearest-neighbor hopping t_1. Notably, the value of the V-O-V angle is surprisingly low (145.5°) in the reported room temperature data of Gitgeatpong *et al.* [10] compared to our work [147.83(19)°] and previous published structural data [147.8(5)° [3], 147.82(7)° [17]]. So in the work of Gitgeatpong *et al.*, the redundancy of the third nearest-neighbor interaction to simulate the experimentally observed susceptibility data presumably lies with the crucial variation of the V-O-V angle. The changes in the structure as well as in the magnitude of the hopping are listed in Table III

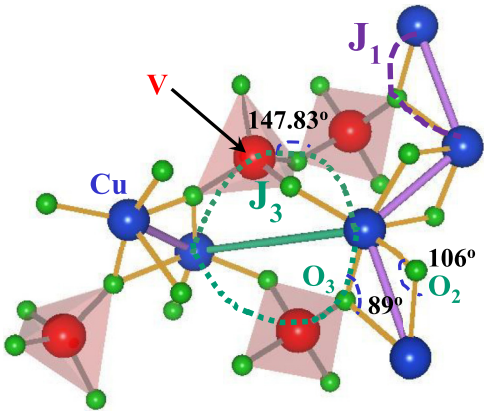

FIG. 5. The path corresponding to the exchange interaction J_1 and J_3 in α-$Cu_2V_2O_7$.

TABLE III. Effect of SOC for the ferromagnetic configuration of the three phases α, β, and γ.

System	Configuration	ΔE/f.u. (meV)	Moment (μ_B/Cu)
	FM+U	0.0	0.71
α-$Cu_2V_2O_7$	FM+SOC+U	−45	0.70
			(0.13)
	FM+U	0.0	0.71
β-$Cu_2V_2O_7$	FM+SOC+U	−40.5	0.70
			(0.08)
	FM+U	0.0	0.71, 0.70
γ-$Cu_2V_2O_7$ [a]	FM+SOC+U	−41.2	0.71, 0.70
			(0.14, 0.14)

[a]Since there are two inequivalent Cu atoms in the system the moments at these two atoms are listed in the table.

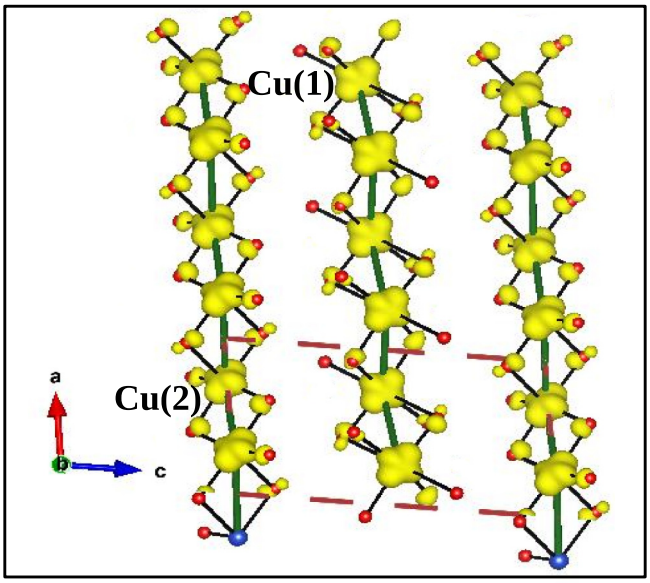

FIG. 6. Electron density plot in the γ phase.

in the SM [14]. Our calculation illustrates the important role of the structure in the magnetic as well as the electronic properties of the sample.

For the γ phase the dominant exchange interaction is J_4 which is AFM (see Table II). Calculation with AMF as DCC, renormalizes the magnitude of the exchange interaction J_4 (−16.9 meV); however, it still remains the strongest interaction leading to the formation of isolated dimers in the γ phase. This is the interaction between the Cu(1) atoms within the chain. Note that t_1 and t_3; t_2 and t_4 are the intrachain hoppings corresponding to the chains formed by Cu(2) and Cu(1), respectively, as shown in Fig. 4(c). For Cu(1) atoms, the exchange interaction J_4 is mediated by two exchange paths, Cu(1)-O(2)-Cu(1) and the double bridges of Cu(1)-O(6)-V(2)-O(1)-Cu(1). These two exchange paths are further visible in the Wannier function plot of Cu-$d_{x^2-y^2}$ and are indicated by a dashed line and a dotted line, respectively in Fig. 4(f). The former path includes the oxygen atom, while the latter path involves the empty (d^0) vanadium atom. The small Cu-O (1.96 Å, 2.00 Å) and V-O (1.65 Å, 1.73 Å) distances in the latter path make J_4 strongest. It is interesting to note for the exchange interaction J_2, the Cu-O (2.42 Å, 2.54 Å) and V-O (1.69 Å,1.84 Å) distances in the exchange path are much larger making the exchange interaction relatively weak. The absence of the V atom in the exchange paths of J_1 and J_3 for the Cu(2) atoms appreciably suppress the exchange interaction, suggesting the important role of V in mediating the exchange interactions.

In the γ phase, the orbitally active Cu^{2+} ions trigger Jahn-Teller distortion of the CuO_5 and CuO_6 polyhedra in such a way that a particular Cu-d state is well separated from the rest. The combination of Q_2 and Q_3 distortion of the $Cu(1)O_6$ octahedra leads the d_{xz} ($d_{x^2-z^2}$) orbital to be magnetically active while the $d_{x^2-y^2}$ orbital is magnetically active for Cu(2). This is further validated by the plot of electron density as shown in Fig. 6. The calculated exchange interactions AFM J_4 and FM J_7 are also found to be consistent with these orbital occupancies.

C. Effect of spin-orbit coupling and estimation of antisymmetric exchange interaction

Finally we have addressed the importance of SOC in these systems. In order to understand the effect of SOC we have considered a ferromagnetic configuration. The total energies of these systems with and without SOC are listed in Table III. The data presented in Table III reveal that there is a substantial gain in energy (∼40–45 meV/f.u.) upon incorporation of SOC with high values of orbital moments (0.08–0.14μ_B) at the Cu site, indicating the important role of SOC in the three phases. With Cu atoms being in d^9 configuration (i.e., more than half filled), spin and orbital moments are aligned in the same direction.

The nearest-neighbor Cu atoms belonging to a chain of α-$Cu_2V_2O_7$ are connected by two bonds Cu-O(2)-Cu and Cu-O(3)-Cu which are structurally asymmetric in nature (see Fig. 5) and hence breaks the inversion symmetry. It is important to note that, in the β and γ phases the bridges connecting the neighboring Cu atoms are symmetric in nature and hence results in an absence of DM interaction in these systems. Thus the absence of inversion symmetry in the presence of SOC can give rise to a noncompensating anisotropic DM-type interaction between the neighboring spins in α-$Cu_2V_2O_7$. In order to investigate the DM interaction for the α phase, we have considered the antisymmetric part of the spin Hamiltonian $H = \sum_{ij} \vec{D}_{ij} \cdot (\vec{S}_i \times \vec{S}_j)$ and calculated the DM interactions parameter ($\vec{D}$) from the total energy calculations in the presence of SOC [31]. We have calculated the three components D_1^x, D_1^y, and D_1^z of the nearest-neighbor DM vector for α-$Cu_2V_2O_7$ by performing LSDA+SOC+U calculations. The details of the calculations are provided in the SM [14]. Our calculated values (in meV) of the components of the nearest-neighbor DM parameter for α-$Cu_2V_2O_7$ are, respectively, $D_1^x = 0.0$, $D_1^y = 1.7$, and $D_1^z = -1.4$. Thus the DM vector is oriented in the yz plane which is also consistent with the ground state magnetic configuration allowed by symmetry as discussed in the next section. The large value of $|\frac{\vec{D}_i}{J_i}|$ (∼0.5) indicates a canted spin structure also evidenced from the small saturation magnetization (∼ 0.08μ_B/f.u.) as observed experimentally [9] from the M-H curve. The DM

interaction also adds to the stabilization of long-range order in the α phase.

D. Ground state magnetic configuration

Finally, we have theoretically investigated the possible magnetic ground state for all the polymorphs of $Cu_2V_2O_7$. For α-$Cu_2V_2O_7$, the magnetic ordering is characterized by the wave vector (0,0,0) as the magnetic order does not alter the conventional unit cell of the crystal [11]. The analysis of the neutron powder diffraction data at 5 K shows that the Cu spins are ordered antiferromagnetically along the a direction with a canting towards the c direction while the moment along the b direction is zero [11]. The wave vector (0,0,0) allows four possible magnetic structures corresponding to the magnetic space groups $Fd'd'2$, $Fd'd2'$ (which corresponds to two magnetic structures depending on the transformation matrix), and $Fdd2$. The details of the symmetry-allowed magnetic structures are given in Table IV of the SM [14]. Our total energy calculation for these magnetic structures shows that the magnetic ground state of the α phase corresponds to the magnetic space group $Fd'd'2$ [shown in Fig. 4(a)] with the spin (orbital) moment of 0.70 (0.15) μ_B/Cu and an energy gap of 1.76 eV. The magnetic space group $Fd'd'2$ allows the z components of the spins to be parallel for all the Cu atoms resulting in a total ferromagnetic component in the system as observed experimentally. The nearest-neighbor Cu atoms [Cu(1) and Cu(4) in Table IV of the SM [14]] in the magnetic ground state corresponding to the magnetic space group $Fd'd'2$ have the x components of the spins as antiparallel, while they have parallel y and z components. Such an orientation of the spins forces the corresponding DM interaction ($\vec{D}_1$) to be on the yz plane as also obtained in our calculation. The symmetry of the magnetic ground state also enforces the second ($\vec{D}_2$) and third ($\vec{D}_3$) neighbor DM interactions to have nonzero x and y components; however, as a consequence of the vanishing y component of the moment ($m_y = 0$) found in experiment, neither $\vec{D}_2$ nor $\vec{D}_3$ can contribute to the spin canting. Therefore the nearest-neighbor DM vector $\vec{D}_1$ can cause a canting along the z direction in agreement with the experiment [11].

Similarly for the β phase, symmetry allows four possible magnetic structures corresponding to the magnetic space groups $C2'/C'$, $C2/C'$, $C2'/C$, and $C2/C$, considering the magnetic unit cell to be similar to the crystallographic conventional unit cell. The details of the magnetic structures corresponding to these magnetic space groups are shown in Table IV of the SM [14]. The total energy calculation shows that the magnetic ground state of the β phase corresponds to the magnetic space group $C2/C'$ [see Fig. 4(b)] with the spin (orbital) moment 0.69 (0.08) μ_B/Cu and an energy gap of 1.78 eV. This magnetic structure does not allow any net magnetic moment as also observed experimentally.

As γ-$Cu_2V_2O_7$ crystallizes in the space group $P\bar{1}$, there are only two allowed magnetic space groups for the system: $P\bar{1}'$ and $P\bar{1}$ assuming that the magnetic cell coincides with the crystallographic unit cell. The magnetic space group $P\bar{1}'$ allows the magnetic moments of the Cu(1) and Cu(2) atoms situated at (x,y,z), $(-x,-y,-z)$ to be directed along (m_x,m_y,m_z) and $(-m_x,-m_y,-m_z)$, respectively. On the other hand, the magnetic space group $P\bar{1}$ allows all the Cu atoms to be ferromagnetically (m_x,m_y,m_z) aligned. The calculated total energy for these two magnetic configurations in the presence of SOC shows that the former configuration $P\bar{1}'$ is lower in energy by 16 meV. In this magnetic configuration, the spin (orbital) moment at the two Cu sites are found to be 0.71 (0.17) and 0.70 (0.12) μ_B, respectively with no net moment. In the magnetic ground state, spin moments have a large component along the y direction with small components along the x and z directions indicating that in the γ phase spins have an easy axis along the y direction. Further, a strong J_4 promotes a system of Cu dimer as indicated in Fig. 4(c). Such a dimeric system is likely to host novel physics. So far, no neutron scattering data exists to understand the magnetic structure of γ-$Cu_2V_2O_7$. Thus our theoretical predictions can be validated by future neutron experiments.

Finally, to estimate magnetocrystalline anisotropy in these systems, we have calculated the total energy difference with respect to the ground state spin configuration by choosing various spin-quantization axes within LSDA+SOC+U. The results of our calculation show that all the polymorphs have anisotropy of easy axis type. While the α and γ phases have easy axis along the y direction, the easy axis for the β phase is found to be along the x direction.

IV. CONCLUSION

Our detailed comparative study of the crystal structure, electronic, and magnetic properties of the three different polymorphs of $Cu_2V_2O_7$ shows the importance of crystal geometry on the magnetic property in all the phases of the compound. In order to understand the magnetic properties of these systems we have calculated the isotropic exchange interaction. These calculations were crucial to identify the dominant exchange paths as well as the relevant spin model for these systems. Our calculations suggest the importance of further neighbor exchange interactions, which are not at all obvious from the structural considerations. Further, we have established a magnetostructural correlation for α-$Cu_2V_2O_7$. We argue that the magnetic property of the α phase is mainly governed by the V-O-V angle and provide a clue to understand the origin of discrepancy in the magnetic properties reported by various groups for this phase. The SOC is found to be important to stabilize the magnetic phases for all these compounds. We find that the lack of inversion symmetry in the α phase allows it to host a sizable DM interaction which in turn not only leads to canting of the spins but also adds to the stability of the long-range magnetic order seen for this system. Finally, assuming that the magnetic unit cell is identical to the crystallographic cell, we have calculated the magnetic ground state for these three phases. The theoretically calculated magnetic ground states of the α and β phases are found to be in agreement with the experimental observations and are consistent with the calculated exchange interactions. While strong interchain interaction J_3 and appreciable DM interaction make the α phase more like a three-dimensional spin system, the β phase is one of the excellent realizations of the two-dimensional honeycomb spin network in agreement with the previous work [4]. On the other hand, the calculation of the isotropic exchange interaction for the γ phase provides

justification for an isolated spin dimer model for this system making it a potential candidate to host spin gap. Further magnetic susceptibility and heat capacity measurements are required to confirm our spin-dimer model for the γ phase. In conclusion, the crystal geometry in the various phases of $Cu_2V_2O_7$ governs the evolution of the spin model for the three phases from the three-dimensional nature in the α phase to the two dimensional in the β phase, while in the γ phase it is isolated spin dimer. Finally, we hope that our detailed study on the different polymorphs of $Cu_2V_2O_7$, showing the important role of crystal structure in determining the magnetic properties, will be helpful for future studies not only on the polymorphs of $Cu_2V_2O_7$ but also broadly for the $M_2X_2O_7$ group.

ACKNOWLEDGMENTS

I.D. thanks Technical Research Centre (TRC), Department of Science and Technology (DST), Government of India for support. S.B. thanks Council of Scientific and Industrial Research (CSIR), India for support through a fellowship.

[1] P. Lemmens, G. Güntherodt, and C. Gros, Phys. Rep. **375**, 1 (2003).
[2] M. Touaiher, K. Rissouli, K. Benkhouja, M. Taibi, J. Aride, A. Boukhari, and B. Heulin, Mater. Chem. Phys. **85**, 41 (2004).
[3] C. Calvo and R. Faggiani, Acta Crystallogr., Sect. B: Struct. Sci., Cryst. Eng. Mater. **31**, 603 (1975).
[4] A. A. Tsirlin, O. Janson, and H. Rosner, Phys. Rev. B **82**, 144416 (2010).
[5] S. V. Krivovichev, S. K. Filatov, P. N. Cherepansky, T. Armbruster, and O. Y. Pankratova, Can. Mineral. **43**, 671 (2005).
[6] G. M. Clark and R. Garlick, J. Inorg. Nucl. Chem. **40**, 1347 (1978).
[7] J. Pommer, V. Kataev, K.-Y. Choi, P. Lemmens, A. Ionescu, Yu. Pashkevich, A. Freimuth, and G. Güntherodt, Phys. Rev. B **67**, 214410 (2003).
[8] M. Sánchez-Andújar, S. Yáñez-Vilar, J. Mira, N. Biskup, J. Rivas, S. Castro-García, and M. A. Señarís-Rodríguez, J. Appl. Phys. **109**, 054106 (2011).
[9] J. Sannigrahi, S. Bhowal, S. Giri, S. Majumdar, and I. Dasgupta, Phys. Rev. B **91**, 220407(R) (2015).
[10] G. Gitgeatpong, Y. Zhao, M. Avdeev, R. O. Piltz, T. J. Sato, and K. Matan, Phys. Rev. B **92**, 024423 (2015).
[11] Y.-W. Lee, T.-H. Jang, S. E. Dissanayake, S. Lee, and Y. H. Jeong, Europhys. Lett. **113**, 27007 (2016).
[12] Z. He and Y. Ueda, Phys. Rev. B **77**, 052402 (2008).
[13] M. Yashima, and R. O. Suzuki, Phys. Rev. B **79**, 125201 (2009).
[14] See Supplemental Material at http://link.aps.org/supplemental/10.1103/PhysRevB.95.075110 for the electronic, structural, and magnetic properties of α, β, and γ-$Cu_2V_2O_7$.
[15] D. Mercurio-Lavaud and B. Frit, C. R. Seances Acad. Sci., Ser. C **277**, 1101 (1973).
[16] J. M. Hughes and M. A. Brown, Neues Jahrb. Mineral., Monatsh. **1989**, 41 (1989).
[17] M. V. Rotermel, T. I. Krasnenko, S. A. Petrova, and R. G. Zakharov, Russ. J. Inorg. Chem. **54**, 22 (2009).
[18] P. E. Blöchl, Phys. Rev. B **50**, 17953 (1994).
[19] G. Kresse and D. Joubert, Phys. Rev. B **59**, 1758 (1999).
[20] G. Kresse and J. Hafner, Phys. Rev. B **47**, 558 (1993).
[21] G. Kresse and J. Furthmüller, Phys. Rev. B **54**, 11169 (1996).
[22] V. I. Anisimov, J. Zaanen, and O. K. Andersen, Phys. Rev. B **44**, 943 (1991).
[23] O. K. Andersen and T. Saha-Dasgupta, Phys. Rev. B **62**, R16219 (2000).
[24] O. K. Andersen, T. Saha-Dasgupta, R. W. Tank, C. Arcangeli, O. Jepsen, and G. Krier, *Electronic Structure and Physical Properties of Solids; The Uses of the LMTO Method*, Springer Lecture Notes in Physics (Springer, Berlin 2000), p. 3.
[25] O. K. Andersen, T. Saha-Dasgupta, and S. Ezhov, Bull. Mater. Sci. **26**, 19 (2003).
[26] A. A. Mostofi, J. R. Yates, Y.-S. Lee, I. Souza, D. Vanderbilt, and N. Marzari, Comput. Phys. Commun. **178**, 685 (2008).
[27] D. I. Khomskii, *Transition Metal Compounds* (Cambridge University Press, Cambridge, UK, 2014).
[28] A. Banerjee, J. Sannigrahi, S. Bhowal, I. Dasgupta, S. Majumdar, H. C. Walker, A. Bhattacharyya, and D. T. Adroja, Phys. Rev. B **94**, 144426 (2016).
[29] P. Blaha, K. Schwarz, P. I. Sorantin, and S. B. Trickey, Comput. Phys. Commun. **59**, 399 (1990).
[30] M. T. Czyzyk and G. A. Sawatzky, Phys. Rev. B **49**, 14211 (1994).
[31] H. J. Xiang, E. J. Kan, S.-H. Wei, M.-H. Whangbo, and X. G. Gong, Phys. Rev. B **84**, 224429 (2011).